JOURNAL OF MATERIALS SCIENCE 14 (1979) 2733–2740

Analytical treatment of the role of surface oxide layers in the sintering of metals

Z. A. MUNIR
Materials and Devices Research Group, Department of Mechanical Engineering, University of California, Davis, CA 95616, USA

The role played by a surface oxide layer in the kinetics of sintering of metallic particles is analysed quantitatively. Application of the analysis to metals with thermodynamically stable oxides gave results which are consistent with experimental observations. The presence of oxides which tend to dissolve in the metal at the sintering temperatures gives rise to an incubation period before the onset of sintering. Comparison with experimental results indicates that the oxide dissolution process is kinetically controlled at the oxide–metal interface.

1. Introduction

Interpretations of the results of sintering investigations have been largely based on models assuming idealized conditions of geometry and purity. Discrepancies between the experimental observations and the theoretical predictions have been commonly attributed to deviations from the assumed conditions in the analyses. Since most metallic powders possess high surface activities, the question of purity becomes of major consequence in practical as well as theoretical considerations. Specifically, since exposure of metallic particles to ambient conditions results nearly always in the formation of an oxide surface layer, established kinetics of pure (one-component) systems cannot be adequately applied to this case.

Various experimental observations have been made on the retardation of (bulk) sintering in the presence of a surface oxide layer [1–3]. In the most recent of these investigations [3], it was demonstrated that the presence of an oxide layer shifts the sintering process from one dominated by a bulk-transport mechanism [4] to that controlled by surface transport [5] with the anticipated lack of densification. Aside from changes in the sintering parameters, other investigations have also reported modifications in the mechanical properties of sintered oxide-coated metallic particles [6–8]. Interpretations of these observations, however, have tended to be qualitative and highly specific. Apparently, there has been no attempt to provide a general, more comprehensive analysis of the sintering kinetics of oxide-coated metallic particles.

The influence exerted by a surface oxide in the sintering of metals is indicated by thermodynamic and kinetic considerations. Conditions can be selected such that the surface oxide is made thermodynamically unstable and hence measured sintering kinetics are those pertaining to the pure metal. Palladium oxide, for example, is unstable at temperatures exceeding 1147 K (at $P_{O_2} \sim$ 1 atm.), or in a conventional vacuum (10^{-4} to 10^{-7} Torr) at lower temperatures. In contrast, thermodynamic calculations show that lead oxide is stable in air and in vacuum in the temperature range of interest, i.e. up to the melting point of the metal. However, in this case reduction of the oxide surface layer can be achieved in a hydrogen atmosphere. These and other metals with similar thermodynamic properties can be sintered free of the oxide under properly selected experimental conditions.

A second group of metals includes those with oxides which are stable with respect to dissociation or reduction (by H_2) but are unstable with respect to dissolution in the parent metal at higher temperatures. At the sintering temperatures, the oxide layer gradually dissolves (as oxygen) in the metal and hence the actual sinter-

0022–2461/79/112733–08 $02.80/0

ing process is preceded by an incubation period dictated by the kinetics of dissolution and diffusion of the oxygen. A third classification includes metals with low oxygen solubility and high oxide stability. The sintering of such metals is preceded by the diffusion of the metal through the oxide layer to the neck region. In this paper we present an analysis of the role played by the surface oxide layer in the sintering of the latter two classes of metals.

2. Mathematical analysis

2.1. Metals with low oxygen solubilities

The basic assumptions involved in the analysis of the sintering of oxide covered metals in this category are (a) complete coverage of the surface of the metal particle by the oxide layer, (b) the dominant mass transport through the oxide layer is bulk diffusion, i.e. short circuit paths, etc., are ignored, and (c) metal–metal sintering is preceded by diffusion of the metal through oxide layer to the neck region. Consider the geometry of two contacting spheres as shown in Fig. 1. The rate of neck growth, $\dot{x}$, is given by

$$\dot{x} = 2D_v F K_1^2 \tag{1}$$

where

D_v = volume diffusion coefficient,
$F = F_s\Omega/kT$,
F_s = surface energy,
Ω = atomic volume,
K_1 = curvature difference for diffusional sources from the surface via volume, surface or evaporation paths

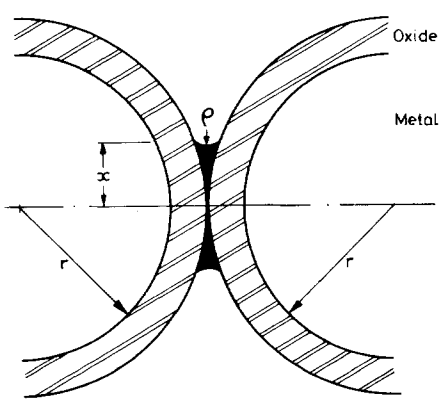

Figure 1 Geometric configuration of sintered oxide-coated spheres.

$$= \left(\frac{1}{\rho} - \frac{1}{x} + \frac{2}{r}\right)\left(1 - \frac{x}{r}\right)$$

and $\rho = x^2/2(r-x)$.

The term $[1-(x/r)]$ in the parameter K_1 is added so that $K_1 = 0$ at $x = r$, i.e. neck growth stops when the neck radius is the same as the particle radius. Equation 1 can now be re-written as

$$\dot{x} = 2\frac{D_v F_s \Omega}{kT}\left[\left\{\frac{2(r-x)}{x^2} - \frac{1}{x} + \frac{2}{r}\right\}\left(1 - \frac{x}{r}\right)\right]^2 \tag{2}$$

and the neck volume rate of growth is

$$\dot{V} = \frac{4\pi}{r} x^3 \dot{x}. \tag{3}$$

Similarly we calculated the atomic flux to the neck region resulting from sintering as

$$\dot{N}_s = \frac{4\pi\rho_0 N_0}{rA_w} x^3 \dot{x} \tag{4}$$

where

ρ_0 = the density of the metal,
N_0 = Avogadro's number, and
A_w = the atomic weight of the metal.

This flux represents a condition of unretarded sintering, i.e. where there is no oxide layer or where the diffusional flux through this layer is equal or greater than $\dot{N}_s$.

Now, in the presence of an oxide layer, unretarded sintering will be attained when the flux through the oxide is equal to that calculated by Equation 4. The flux through the oxide layer is

$$\dot{N}_d = J(2\pi x^2) \tag{5}$$

where the expression $(2\pi x^2)$ represents the area of the metal–oxide interface on both sides of the neck, and J is the diffusional flux per unit area of interface. Assuming a time-independent concentration gradient of the metal in the oxide layer, Equation 5 can be rewritten as

$$\dot{N}_d = 2\pi x^2 \left|\frac{\Delta C}{\xi}\right| D_x \tag{6}$$

where ΔC = the concentration difference of the metal across the oxide layer, ξ = the oxide thickness and D_x = the diffusion coefficient of the metal through the oxide.

As stated earlier, unretarded sintering occurs when $\dot{N}_s = \dot{N}_d$, i.e.

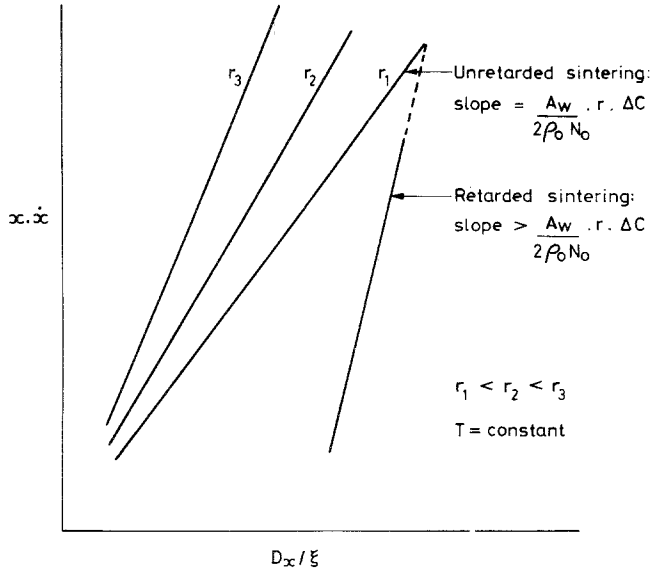

Figure 2 Geometric configuration for a metal with high oxygen solubility.

$$x\dot{x} = \frac{A_w}{2\rho_0 N_0} r\Delta C \frac{D_x}{\xi} \tag{7}$$

A plot of $x\dot{x}$ versus D_x/ξ gives a straight line with a slope of $(A_w/2\rho_0 N_0)r\Delta C$, as shown in Fig. 2. Also shown in Fig. 2 is a line representing the results of a case where sintering is retarded by the slow diffusion of the metal through the oxide layer. For any given oxide thickness and temperature, the rate of neck growth increases with increasing particle size for unretarded sintering. This is shown qualitatively in Fig. 2. Also, since $(x\dot{x})$ is directly proportional to ΔC, the dependence of the latter parameter on P_{O_2}, the partial pressure of oxygen, will influence the growth rate. The dependence of ΔC on pressure is of the form

$$\Delta C = k(\Delta P_{O_2})^{1/n}, \tag{8}$$

where ΔP_{O_2} is the difference between the oxygen partial pressure at oxide–gas interface and the dissociation pressure of the oxide, and n and k are constants ($n = 4$ for the Cu/Cu_2O system, for example).

Once a neck is formed then the kinetics become governed by two equations, one describing the neck growth due to unretarded sintering and the second describes the neck growth rate as controlled by diffusion through the oxide layer. These relationships are, respectively,

$$\dot{x}_s = \frac{2D_v F_s \Omega K_1^2}{kT} \tag{9}$$

and

$$\dot{x}_d = \frac{2\bar{D}F_s' \Omega K_1^2}{kT} \tag{10}$$

where F_s' represents a surface energy modified by the presence of the oxide layer, and

$$\bar{D} = \frac{D_v D_x (r + \xi)}{rD_x + \xi D_v} \tag{11}$$

Thus using the approximation that $F_s' \sim F_s$, we can relate Equations 9 and 10 as follows:

$$\frac{\dot{x}_s}{\dot{x}_d} = \frac{D_x + \xi/rD_v}{D_x(1 + \xi/r)} \tag{12}$$

However, since $\xi \ll r$, Equation 12 can be simplified to

$$\frac{\dot{x}_s}{\dot{x}_d} \simeq 1 + \xi/r \frac{D_v}{D_x} \tag{13}$$

which gives $\dot{x}_s/\dot{x}_d \simeq 1$ when $D_v = D_x$, i.e. when the diffusivities of the metal atoms in the oxide and in the metal itself are the same. When $D_v \gg D_x$, Equation 13 becomes

$$\frac{\dot{x}_s}{\dot{x}_d} \simeq (\xi/r) \frac{D_v}{D_x} \tag{14}$$

and when $D_x \gg D_v$ then the rate ratio becomes essentially unity.

2.2. Metals with high oxygen solubilities

In this case we are dealing with a metal whose oxide surface layer becomes unstable with respect to an oxygen saturated metal at the sintering

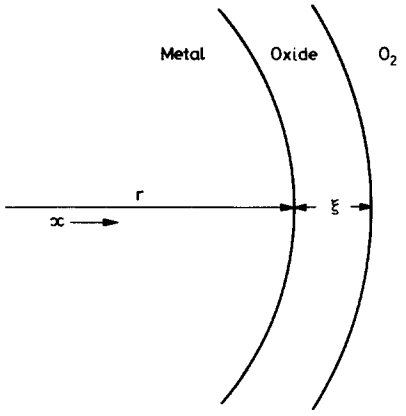

Figure 3 Geometric configuration for a metal with high oxygen solubility.

temperature. Referring to Fig. 3, we make the following definitions and simplifying assumptions:

(a) the concentration of O in M at $x = r$ is C_m which is the solubility limit of O in M at the experimental temperature;

(b) $\xi \ll r$;

(c) the concentration of O in the oxide is constant, and

(d) the initial concentration of O in M is assumed to be zero.

For any given metallic particle size, r, there is a maximum amount of oxide which can be dissolved into the particle, i.e. there is a maximum ξ. For thicknesses greater than this maximum, the oxide cannot dissolve entirely and the role of the remaining layer can be determined along the lines of the analysis presented above. In order to calculate this maximum ratio of (ξ/r) we define

V_x = the total volume of the oxide
V_m = the total volume of the metal

and

C_x = the concentration of the oxygen in the oxide.

Therefore, for maximum uptake of oxygen

$$C_m V_m = V_x C_x \quad (15)$$

or

$$R_c^3 + 3R_c^2 + 3R_c = C_m/C_x \quad (16)$$

where $R_c \equiv (\xi/r)$ max, the critical ratio. Since $\xi \ll r$, the term R_c^3 can be ignored and the solution to the above equation becomes

$$R_c = \frac{1}{2}\left[\left(1 + \frac{4}{3}\frac{C_m}{C_x}\right)^{1/2} - 1\right] \quad (17)$$

The assumption that R_c^3 is negligible introduces an error of about 5% for ξ/r values of up to 0.5. In fact for low ξ/r, i.e. $\leqslant 0.1$, the following relationship can be used with an accuracy of $\lesssim 9\%$:

$$R_c \simeq \frac{1}{3}\frac{C_m}{C_x} \quad (18)$$

Since $C_x \simeq$ independent of temperature, R_c increases with increasing temperature.

At the critical ξ/r ratio (i.e. at R_c) the time necessary to diffuse the oxygen (from the oxide layer) into the metallic sphere can be calculated from [9]:

$$\frac{C - C_1}{C_s - C_1} = 1 + \frac{2r}{\pi x}\sum_{n=1}^{\infty}\frac{(-1)^n}{n}\sin\frac{n\pi x}{r} \times \exp(-Dn^2\pi^2 t/r^2) \quad (19)$$

where C_1 = initial concentration of O in the metal, D = diffusion coefficient of O in the metal, t = time, and C_s = the surface concentration. For the moment we shall assume that $C_s = C_m$, i.e. that the dissolution reaction of the oxide

$$MO_2 = M + 2O \text{ (dissolved)} \quad (20)$$

is not kinetically hindered. In other words, we assume that the oxygen concentration at $x = r$ remains constant (as long as there is an oxide) at a value of C_m. The significance of this assumption will be discussed later.

As $x \to 0$, i.e. at the centre of the sphere, Equation 19 simplifies [9] to

$$\frac{C - C_1}{C_m - C_1} = 1 + \sum_{n=1}^{\infty}(-1)^n \exp(-Dn^2\pi^2 t/r^2) \quad (21)$$

which, for a saturated sphere [10] gives

$$Dt/r^2 \simeq 0.6 \quad (22)$$

where r is the radius of the sphere corresponding to the (critical) R_c value. Thus the incubation period before the onset of sintering can be calculated from Equation 22 for particles with the maximum oxide thickness.

3. Discussion

For metals with low oxygen solubility and high oxide stability, determination of the role of the surface oxide layer in the sintering kinetics can be made by the application of Equation 12. When the calculated values of the rate ratios, $\dot{x}_s/\dot{x}_d$,

TABLE I Self and oxide diffusivities of metals in their sintering range

Metal	T (K)	D_v(m^2 sec^{-1})	D_x(m^2 sec^{-1})	References*
Al	467	2.07×10^{-20}	1.24×10^{-56}	[11, 12]
	933	1.84×10^{-12}	5.51×10^{-30}	
Co	883	1.44×10^{-21}	4.96×10^{-17}	[13, 14]
	1765	3.42×10^{-13}	2.85×10^{-12}	
Cr	1038	6.04×10^{-21}	3.69×10^{-22}	[15, 16]
	2176	7.90×10^{-13}	3.70×10^{-11}	
Cu	678	4.10×10^{-21}	1.01×10^{-17}	[17, 18]
	1356	5.65×10^{-13}	6.65×10^{-12}	
Fe	906	1.53×10^{-18}	8.04×10^{-13}	[19, 20]
	1812	2.88×10^{-11}	3.14×10^{-9}	
Mg	462	6.30×10^{-20}	1.21×10^{-42}	[21, 22]
	923	3.01×10^{-12}	5.25×10^{-24}	
Ni	863	1.14×10^{-21}	2.66×10^{-20}	[23, 24]
	1726	4.66×10^{-13}	3.57×10^{-14}	
Pb	300	2.25×10^{-23}	8.76×10^{-48}	[25, 26]
	600	4.47×10^{-14}	9.36×10^{-24}	
U	703	3.24×10^{-16}	6.77×10^{-33}	[27, 28]
	1406	8.68×10^{-12}	5.20×10^{-22}	
Zn	347	5.94×10^{-20}	2.88×10^{-16}	[29, 30]
	693	1.01×10^{-12}	2.73×10^{-12}	

*The first of each set of two references refers to the self-diffusivity of the metal and the second is the reference for the diffusivity of the metal through its own oxide.

are larger than unity a retardation of sintering is predicted. Conversely, values of $\dot{x}_s/\dot{x}_d \leqslant 1$ signify a transport process that is unaffected by the presence of the surface layer. Utilizing reported diffusion data (Table I) ratios of $\dot{x}_s/\dot{x}_d$ were calculated for several metals and are shown in Table II. These ratios were determined for ξ/r values ranging from 10^{-5} to 10^{-1} and at $0.5\,T_m$ and T_m, where T_m is the absolute melting point of the metal. The range of temperature delineated by these two values covers the experimental sintering region. The results shown in Table II predict that the presence of an oxide layer makes essentially no difference in the kinetics of sintering of such metals as chromium, cobalt, copper, iron, nickel, and zinc. On the other hand, the exceedingly large values of $\dot{x}_s/\dot{x}_d$ calculated for aluminium, magnesium, lead, and uranium indicate that the sintering process of these metals is retarded by the presence of an oxide surface layer. For these metals retardation is predicted even at the lowest ξ/r ratio listed in Table II.

The predictions of the present analysis concerning the effect of a stable oxide surface layer on the kinetics of sintering of metals are consistent with experimental observations. Oxide coated particles of aluminium [31] and lead [3] showed no densification when sintered at temperatures approaching the melting points of the metals. In contrast when the oxide is rendered thermodynamically unstable (in the case of lead) sintered powder compacts showed substantial densification at temperatures considerably lower than the melting point. Similar observations have been made on palladium [2]. In addition, the predicted passive role of the surface layer in the sintering of such metals Cu, Fe and Ni is also in agreement with experimental observations. The investigations of Ramakrishnan and Tendolkar [6, 7] have shown that the sintering of these metals is unretarded by the presence of oxide surface layers of up to 1200 Å thick. The observed enhancement of sintering, concluded from densification data, is believed to be the result of grain growth retardation brought about by the presence of the oxide phase at the grain boundaries [32].

The more recent observations of Heath and Evans [8] offer further evidence of the sinterability of oxide-coated copper particles. Scanning electron microscopic records gave clear indications of neck formation between spheres and between spheres and the underlying copper foils.

TABLE II Neck growth rate ratios, $\dot{x}_s/\dot{x}_d$, for metals in their sintering range

Metal	T (K)	ξ/r		
		10^{-5}	10^{-3}	10^{-1}
Al	467	1.67×10^{31}	1.67×10^{33}	1.52×10^{35}
	933	3.3×10^{12}	3.3×10^{14}	3.0×10^{16}
Co	833	1.0	1.0	0.91
	1765	1.0	1.0	0.92
Cr	1038	1.0	1.0	2.40
	2176	1.0	1.0	0.91
Cu	678	1.0	1.0	0.91
	1356	1.0	1.0	0.92
Fe	906	1.0	1.0	0.87
	1812	1.0	1.0	0.91
Mg	462	5.20×10^{17}	5.20×10^{19}	4.7×10^{21}
	923	5.7×10^{6}	5.7×10^{8}	5.2×10^{10}
Ni	863	1.0	1.0	0.91
	1726	1.0	1.0	2.1
Pb	300	2.6×10^{19}	2.6×10^{21}	2.3×10^{23}
	600	4.8×10^{4}	4.8×10^{6}	4.3×10^{8}
U	703	4.8×10^{11}	4.8×10^{13}	4.4×10^{15}
	1406	1.7×10^{5}	1.7×10^{7}	1.5×10^{9}
Zn	347	1.0	1.0	0.91
	693	1.0	1.0	0.94

Neck formation was observed between contacting, but uncompacted particles of copper heated at 850° C for as little as 2 min. Moreover, fracture surfaces of the neck regions showed two distinct morphologies resembling those of brittle and ductile fracture. Heath and Evans [8] interpreted these observations in terms of a sintering process that is initiated by the diffusion of copper through the oxide layer to the neck region.

If the oxygen solubility in a metal at the sintering temperature is appreciable, the dissolution of the oxide layer is possible and its duration would represent an incubation period before the onset of sintering. Experimental evidence for such a process is provided by the work of Watanabe and Hirokoshi on titanium [31]. These authors reported that titanium powder coated with an approximately 100 Å thick oxide layer sintered after a 60 min anneal at 1000° C. Although no other sintering study has dealt specifically with this topic, the concept of an incubation period is supported by annealing experiments on oxide-coated copper films [33]. In order to assess the kinetics of the pre-sintering process we must first calculate the maximum oxide thickness that can dissolve in a given particle size. The ratio of oxide thickness to particle radius representing the maximum is calculated from Equation 17. Results of these calculations are given in Table III. The temperatures listed in this table represent conditions at which solubility limits are reported [34]. In one case (Pb) the only available solu-

TABLE III Calculations of the critical oxide thickness to particle radius ratios, R_c

Metal	T (K)	C_m (kg m^{-3})	C_x (kg m^{-3})	R_c
Al	873	1.08	1.87×10^{3}	1.92×10^{-4}
Co	1148	1.82	1.38×10^{3}	4.38×10^{-4}
Cu	1323	6.90×10^{-1}	6.71×10^{2}	3.42×10^{-4}
Fe	1623	1.97×10^{-1}	1.27×10^{3}	5.14×10^{-5}
Ni	1473	1.07	1.43×10^{3}	2.49×10^{-4}
Pb	600	6.12×10^{-2}	6.83×10^{2}	2.98×10^{-5}
Ti	> 1273	5.85×10^{2}	1.71×10^{3}	1.03×10^{-1}

TABLE IV Pre-sintering incubation periods

Metal	T(K)	r_c(m)	D (m^2 sec^{-1})	t_i(sec)
Al	873	5.21×10^{-5}	$\sim 10^{-17}$	$\sim 10^{7}$
Cu	1323	2.92×10^{-5}	2.11×10^{-13}	2.42×10^{3}
Fe	1623	1.94×10^{-4}	2.12×10^{-9}	10.7
Ti	1273	9.71×10^{-8}	9.60×10^{-13}	5.87×10^{-3}

bility information is for the molten state and is assumed in the present calculations as an approximation for the appropriate solid state data near the melting point. The time necessary for the dissolution of the oxide is calculated from Equation 22 with r being the critical radius for a 100 Å thick oxide layer. The results of such calculations are given in Table IV for aluminium, copper, iron and titanium. According to these results the incubation period, t_i, preceding sintering is insignificant in the cases of Fe and Ti, and appreciable in the case of Cu ($\sim$40 min). Because of the absence of diffusion data for oxygen in aluminium the value listed in Table IV is only an estimate. Since oxygen is present in molten aluminium as an oxide [34], we estimate the diffusion coefficient of oxygen in solid aluminium to be of the same order of magnitude as that of the slowest moving metals in Al, i.e. $\sim 10^{-17}$ m^2 sec^{-1}. From this value we calculate t_i for a 100 Å thick oxide layer on a particle with the critical radius to be $\sim 10^7$ sec ($\sim$116 days).

Only two experimental investigations provide information which can be discussed in light of the calculations of t_i. Watanabe and Hirokoshi [31] estimated a t_i for oxide-coated Ti particles to be about 60 min. This value is several orders of magnitude larger than that listed in Table IV. The discrepancy between the experimental value and the calculated one clearly indicates that the assumed absence of a kinetically controlled step in the dissociation of the oxide, Equation 20, is not valid in this case. In other words, the concentration of oxygen in the titanium particle at $x = r$ see (Fig. 3) is less than C_m, the solubility limit. The second pertinent observation is that of Heath and Evans [8]. Copper oxide particles were present after sintering at 850° C for up to 135 min. As in the case of titanium, the time predicted in the present analysis is much shorter than that based on experimental observations. The concept of a kinetic barrier to oxide dissolution is probably related to the coherence of the oxide–metal boundary, and has an analogy in low stress creep of oxide–metal dispersions [35].

Acknowledgements

Appreciation is extended to the management of the Berkeley Nuclear Laboratory (Gloucestershire, England) for providing the author with a stimulating environment during a sabbatical leave. The financial support from the Lawrence Livermore Laboratory (Livermore, California) during the early part of this work is gratefully acknowledged. Special thanks are extended to W. B. Beeré and M. V. Speight of BNL, and to R. Condit and B. J. Holt of LLL for helpful discussions and critical comments.

References

1. R. F. SMART and E. C. ELLWOOD, *Nature* **181** (1958) 833.
2. H. U. ANDERSON, *Sci. Sintering* **6** (1974) 45.
3. R. K. HIGGINS and J. A. MUNIR, *Powder Met.* (1979) in press.
4. R. M. GERMAN and Z. A. MUNIR, *Met. Trans.* **6A** (1975) 2229.
5. *Idem, ibid* **6B** (1975) 289.
6. P. RAMAKRISHNAN and G. S. TANDOLKAR, *Powder Met.* **1** (1964) 34.
7. P. RAMAKRISHNAN, *ibid.* 9 (1966) 47.
8. P. J. HEATH and P. E. EVANS, *J. Mater. Sci.* 9 (1974) 1955.
9. J. CRANK, "The Mathematics of Diffusion", 2nd edn (Oxford University Press, Oxford, 1975) p. 91.
10. H. S. CARSLAW and J. C. JAEGER, "Conduction of Heat in Solids", 2nd edn (Oxford University Press, Oxford, 1959) p. 102.
11. T. S. LUNDY and J. F. MURDOCK, *J. Appl. Phys.* **33** (1962) 1671.
12. A. E. PALDINO and W. D. KINGERY, *J. Chem. Phys.* **37** (1962) 957.
13. H. W. MEAD and C. E. BIRCHENALL, *Trans. Met. Soc. AIME* **203** (1955) 994.
14. W. K. CHEN, N. L. PETERSON and W. T. REEVES, *Phys. Rev.* **186** (1969) 887.
15. J. ASKILL and D. H. TOMLIN, *Phil. Mag,* **11** (1965) 467.
16. R. LINDER and A. AKERSTRÖM, *Z. Phys. Chem. N.F.* **6** (1956) 162.
17. S. J. ROTHMAN and N. L. PETERSON, *Phys. Stat. Sol.* **35** (1969) 305.
18. W. J. MOORE and B. SELIKSON, *J. Chem. Phys.* **19** (1951) 1539.
19. R. ANGERS and F. CLAISSE, *Can. Met. Q.* **1** (1968) 73.

20. L. HIMMEL, R. F. MEHL and C. E. BIRCHENALL, *Trans. AIME* **197** (1953) 822.
21. P. G. SHEWMON, *Trans. Met. Soc. AIME* **206** (1956) 918.
22. R. LINDER and G. D. PARFITT, *J. Chem. Phys.* **26** (1957) 182.
23. K. MONMA, H. SUTO and H. OIKAWA, *J. Jap. Inst. Met.* **28** (1964) 188.
24. S. M. KLOTSMAN, A. N. TIMOFEYEV and I. S. TRAKHTENBERG, *Fiz. Metal. Metalloved.* **14** (1962) 428.
25. J. W. MILLER, *Phys. Rev.* **181** (1969) 1905.
26. R. LINDER, *Arkiv Kemi* **4** (1952) 385.
27. S. J. ROTHMAN, L. T. LLOYD and A. L. HARKNESS, *Trans. Met. Soc. AIME* **218** (1960) 605.
28. R. J. HAWKINS and C. B. ALCOCK, *J. Nucl. Mater.* **26** (1968) 112.
29. N. L. PETERSON and S. J. ROTHMAN, *Phys. Rev.* **163** (1967) 645.
30. D. G. THOMAS, *J. Phys. Chem. Solids* **3** (1957) 229.
31. H. WATANABE and Y. HORIKOSHI, *Int. J. Powder Met. & Tech.* **12** (1976) 209.
32. M. F. ASHBY and M. A. CENTAMORE, *Acta Met.* **16** (1968) 1081.
33. D. B. RAO, K. HEINEMANN and D. L. DOUGLASS, *Oxid. of Met.* **10** (1976) 227.
34. C. J. SMITHELLS, "Metals Reference Book" (Butterworths, London, 1967).
35. W. VICKERS and P. GREENFIELD, *J. Nucl. Mater.* **27** (1968) 73.

Received 28 March and accepted 26 April 1979.